ISSN 1063-7826, Semiconductors, 2018, Vol. 52, No. 14, pp. 1882–1885. © Pleiades Publishing, Ltd., 2018.

GRAPHENE

High Quality Graphene Grown by Sublimation on 4*H*-SiC (0001)[1]

A. A. Lebedev[a], V. Yu. Davydov[a,*], D. Yu. Usachov[b], S. P. Lebedev[c], A. N. Smirnov[a], I. A. Eliseyev[a], M. S. Dunaevskiy[a], E. V. Gushchina[a], K. A. Bokai[b], and J. Pezoldt[d]

[a] *Ioffe Institute, St. Petersburg, 194021 Russia*
[b] *Saint Petersburg State University, St. Petersburg, 199034 Russia*
[c] *ITMO University, St. Petersburg, 197101 Russia*
[d] *Technische Universität Ilmenau, Ilmenau, 98693 Germany*
**e-mail: valery.davydov@mail.ioffe.ru*

Abstract—The structural and electronic characteristics of epitaxial graphene films grown by thermal decomposition of the Si face of a semi-insulating 4*H*-SiC substrate in an argon environment have been studied by a large set of analytical techniques. It is shown that the results of a complex study make it possible to optimize the growth parameters and develop a reliable technology for the growth of high-quality single-layer graphene films. The charge-carrier concentration in the graphene layer was within 7×10^{11}–1×10^{12} cm^{-2}, and the maximum mobility of electrons at room temperature approached 6000 cm^2/(V s).

DOI: 10.1134/S1063782618140154

1. INTRODUCTION

The most promising technology of graphene synthesis, which provides the formation of high-quality material and can be integrated into commercial production technology, is believed to be that based on the thermodestruction of semi-insulating silicon carbide (SiC) substrates [1]. This technology allows formation of graphene on surfaces of commercial SiC substrates with a diameter of up to 6 inches that are produced by the industry at present. Structures of this kind can be used in the standard technological line for the fabrication of semiconductor devices. It is known that the morphological and structural characteristics of graphene films grown on the Si face of SiC are more favorable for the development of devices on their basis.

The goal of our study is the systematic diagnostics of graphene films produced by thermal decomposition of the Si face of a 4*H*-SiC substrate in order to relate the structural and electronic characteristics of the films to the technological growth parameters.

2. EXPERIMENTAL

To obtain graphene films, we used the modified growth technique in an inert gas (argon), which enables more precise control over the sublimation of silicon-carbide components. As a consequence, it is possible to control with high precision both the growth process of a graphene film and the uniformity of coating a substrate with graphene. The growth temperature was about 1800°C and the substrates were high-resistance SiC substrates of the 4*H* polytype with the orientation (0001) (Si face). The structural, chemical, and electronic characteristics of the graphene being grown were measured by Raman spectroscopy, atomic-force microscopy (AFM), Kelvin-probe microscopy, low-energy electron diffraction (LEED), X-ray photoelectron spectroscopy (XPS), angle-resolved photoemission spectroscopy (ARPES), and near-edge (*K*-edge of carbon) X-ray absorption fine structure spectroscopy (NEXAFS).

3. RESULTS AND DISCUSSION

Below results that are typical of samples grown in the final stage of optimization of the technological parameters are presented.

Figure 1 shows an array of Raman spectra measured on a sample area of 10×10 μm^2. The total number (N) in the array is 121 spectra. The spectra show features appearing upon light scattering from the graphene film: *G* and 2*D* lines and a weak *D* line [2]. Analysis of the *G* line intensity map, which was obtained by processing this array, revealed a rather uniform distribution of the line intensity over the sample area. This is indicative of good thickness uniformity of the graphene film in the region being analyzed. It was found that the 2*D* line is symmetric in the majority of spectra and is well fitted by a single Lorentzian, which is a sign of single-layer graphene [2]. The shape of the 2*D* line which can be approximated by an envelope of four Lorentzians is observed

[1] The article is published in the original.

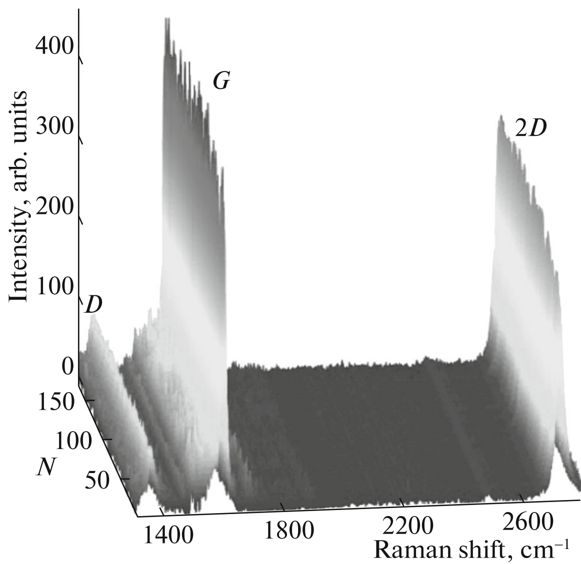

Fig. 1. Array of Raman spectra for a sample grown on the Si face of 4H-SiC. The contribution of the substrate spectrum is subtracted from the original array of spectra.

in no more than 10% of the total number of spectra in the array. It follows from the analysis of 2D line shape that the sample is mostly formed by single-layer graphene with a small number of double-layer inclusions. The ratio between the integral intensities of D and G lines (I_D/I_G) can be used to evaluate the structural perfection of a graphene film. It was found that the I_D/I_G ratio distribution has a maximum at around 0.08–0.09, which corresponds to a defect concentration of $N_d < 10^{10}$ cm^{-2} [3]. The in-plane compressive strain in the graphene layer estimated from the correlation between the positions of the G and 2D lines is $\varepsilon_{\parallel} = (0.30 \pm 0.03)\%$.

The image of the surface potential distribution obtained by Kelvin-probe microscopy (Fig. 2a) shows light regions (regions of increased potential) in the form of elongated strips whose direction coincides with that of the terraces in the topographic image. The area of the light regions does not exceed 10% of the image area. It was found that the potential difference between the light and dark regions is 120 mV (Fig. 2b). This value corresponds to the difference between the surface potentials of single and double-layer graphene [4]. The light regions in Fig. 1a are identified as double-layer graphene. This conclusion agrees with the results of Raman studies of the same sample area.

The LEED pattern demonstrates a $(6\sqrt{3} \times 6\sqrt{3})R30°$ structure characteristic of the graphene/SiC(0001) sample. This structure appears because of the lattice mismatch between graphene and the SiC (0001) surface. No other ordered carbon phases were found in the LEED pattern. The distinct reflections are indicative of the strict spatial orientation of the graphene lattice.

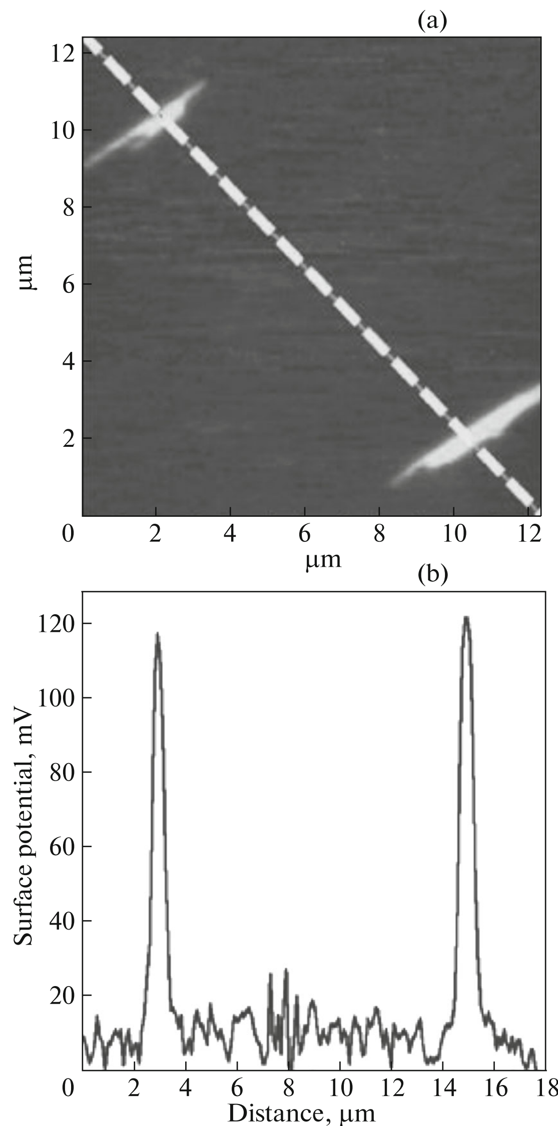

Fig. 2. (a) Surface potential distribution for a sample grown on the Si face of 4H-SiC. (b) Surface potential profile taken along the dashed line on Fig. 2a.

To determine the chemical composition of the near-surface region, a survey XPS spectrum was measured upon removing molecules adsorbed in air via heating in ultrahigh vacuum at a temperature of 500°C. Only a small amount of oxygen was found in the spectrum in addition to lines related to carbon and silicon and peaks associated with the characteristic loss of energy by electrons. The content of oxygen in the upper atomic layers of SiC is approximately 1 at %.

A detailed analysis of the shape of the XPS data in the region of the C 1s line makes it possible to estimate the average graphene thickness. To reliably determine the thickness of graphene, we analyzed XPS spectra obtained at three photon energies providing different depths of analysis within the range from 5 to 12 Å

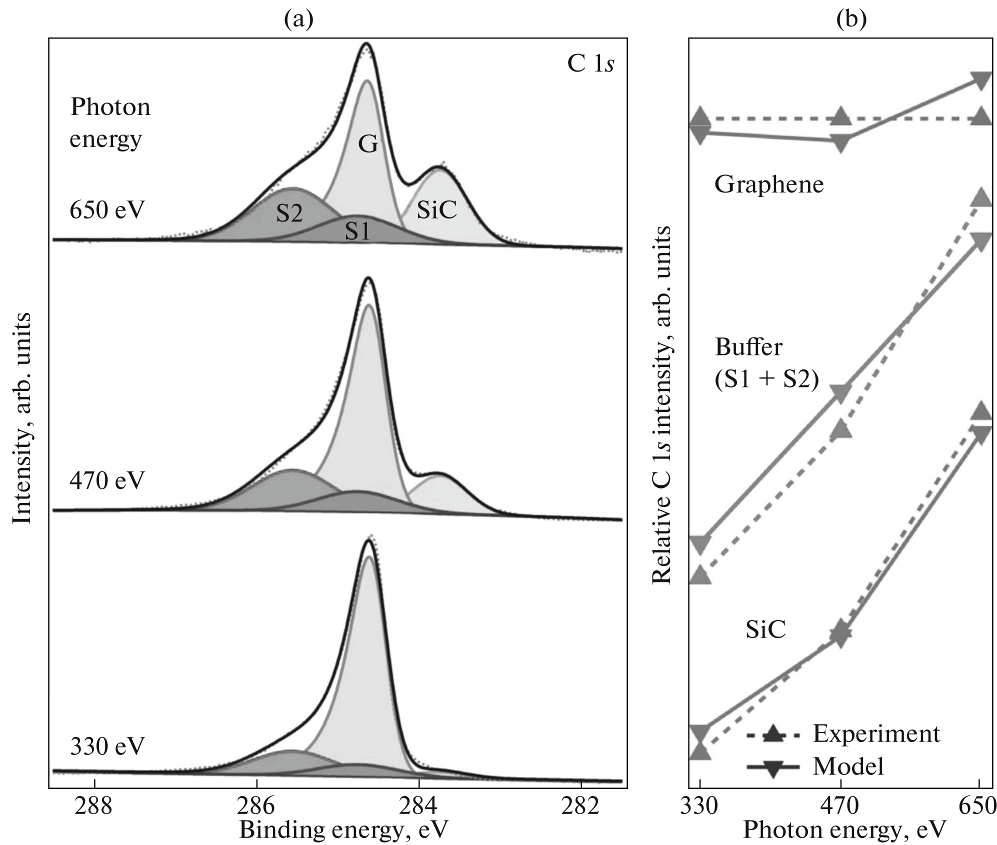

Fig. 3. (a) XPS spectra measured in the C 1*s* region at various photon energies. (b) Result of simulation of the intensities of spectral components.

(Fig. 3a). The layer thicknesses were determined by choosing those thicknesses of the graphene and buffer layer that provided the best coincidence between the calculated and measured intensities of separate components of C 1s spectra. The results obtained are presented in Fig. 3b, which shows the relative intensities for the optimal thicknesses: 4.5 Å for the buffer layer and 5.7 Å for graphene. This corresponds to 1.5 and 1.7 layers of sp^2 carbon for the buffer layer and graphene, respectively.

It is known that the electronic structure of the valence band varies with the number of graphene layers. Single-layer graphene is characterized by a Dirac cone of electronic states at point *K* of the Brillouin zone, whereas the formation of a second layer leads to energy splitting of the cone and to doubling of the number of states. The ARPES data for the electronic structure of the valence band of the graphene/SiC(0001) heterostructure are shown in Fig. 4. An unsplit Dirac cone is seen at point K. This indicates that a single-layer graphene coating is predominant on the surface. A weak tiny feature at 0.27 eV indicates presence of bilayer regions. This conclusion agrees with the Raman and AFM data, according to which a single-layer graphene with a small amount (~10%) of inclusions of double-layer islands with submicrometer dimensions was formed. However the graphene thickness determined by XPS is higher than the values obtained by other methods probably due to elastic scattering of photoelectrons, which was neglected in our analysis.

A convincing demonstration of the fact that both graphene and the buffer layer are constituted by planar sp^2 structures is provided by NEXAFS. Figure 5 shows NEXAFS spectra recorded in the partial-quantum-yield mode. A characteristic feature of the absorption spectra of graphene-like structures is the presence of π- and σ-resonances having opposite angular dependences. The intensity of the σ-resonance is expected to be at a maximum when the polarization vector of photons lies in the graphene plane (angle 0°). In this case, the intensity of the π-resonance must tend to zero. A dependence of this kind is observed in Fig. 5 and indicates that graphene and the buffer layer are planar sp^2 structures oriented parallel to the SiC surface. However, the intensity in the region of the π resonance does not fully disappear at an angle of 0°. This is accounted for by the nonzero contribution to the spectra from the absorption edge of SiC, or it may also be indicative of slight corrugation of the sp^2 layers as a result of their interaction with the substrate.

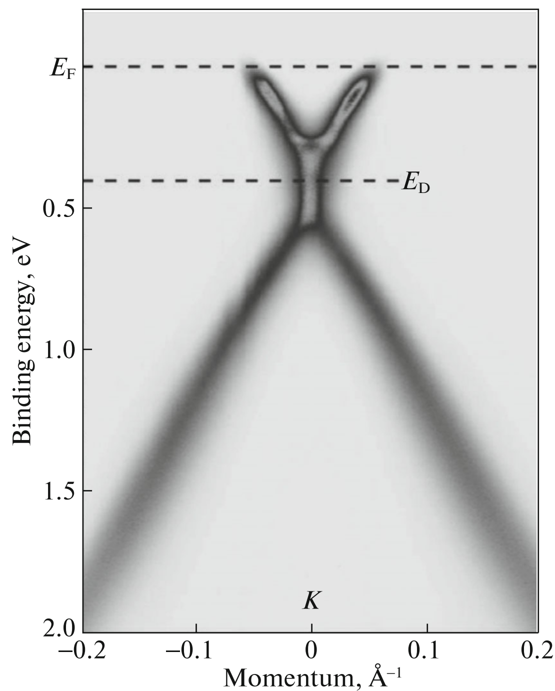

Fig. 4. Electronic structure of the valence band in the vicinity of point *K* of the Brillouin zone. The momentum axis is perpendicular to the ΓK direction. The ARPES data were obtained at photon energy of 40 eV and at temperature of 30 K.

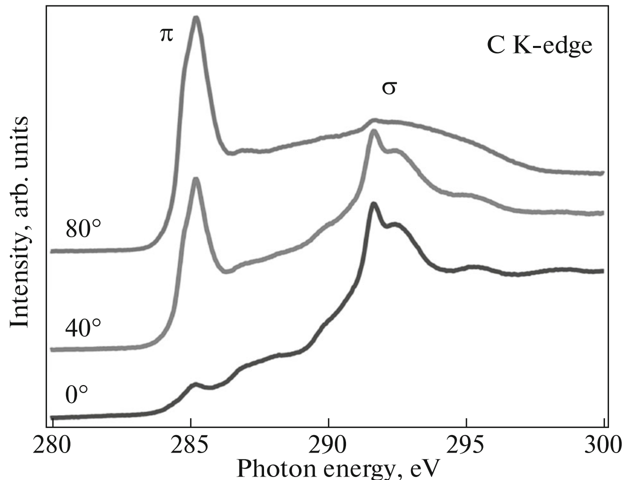

Fig. 5. NEXAFS spectra. The angle between the sample surface and the vector of photon linear polarization is given above the spectra.

Graphene-film samples for electrical measurements were prepared by forming test structures with Hall-bar geometry. The concentration and mobility of charge carriers in graphene were measured at room temperature on a HL550PC (Accent Optical Co., UK) setup at a magnetic field of 0.314 T. The sign of the observed Hall response signal was indicative of electron (n) type conduction. Concentration Q of carriers in the two-dimensional electron gas (2DEG) in graphene was within 7×10^{11}–1×10^{12} cm^{-2}, and the maximum mobility of electrons (μ_{max}) in the obtained graphene films reached about 6000 cm^2/(V s). Note that the values of mobility in graphene films with electron concentrations below 1×10^{12} cm^{-2} obtained in the present work are close to theoretical values calculated for graphene films with intrinsic conductivity at $T = 300$ K on the Si face of SiC in the absence of intercalated hydrogen [5].

4. CONCLUSIONS

It may be concluded that the method of thermodestruction of 4*H*-SiC (0001) surface in argon under selected technological conditions (argon pressure, 700–760 Torr; growth temperature, 1800–1850°C; growth time, 10 min; sample heating rate, 100–150°C/min) can be used for obtaining high-quality single-layer graphene films possessing carrier mobilities close to values theoretically predicted for graphene films with intrinsic conductivity on the Si face of SiC. These results open the possibility of using the proposed technology in the fabrication of graphene-based devices.

ACKNOWLEDGMENTS

D.Yu.U. and K.A.B. acknowledge Saint Petersburg State University for research Grant no. 11.65.42.2017 and RFBR (grant no. 17-02-00427). S.P.L. acknowledges support by the Grant for Young Scientists and Postgraduates from the President of the Russian Federation, order no. 1684 of December 30, 2016.

REFERENCES

1. K. V. Emtsev, A. Bostwick, K. Horn, J. Jobst, G. L. Kellogg, L. Ley, J. L. McChesney, T. Ohta, S. A. Reshanov, J. Rohrl, E. Rotenberg, A. K. Schmid, D. Waldmann, H. B. Weber, and T. Seyller, Nat. Mater. **8**, 203 (2009).
2. A. C. Ferrari and D. M. Basko, Nat. Nanotechnol. **8**, 235 (2013).
3. R. Beams, L. G. Cancado, and L. Novotny, J. Phys.: Condens. Matter **27**, 083002 (2015).
4. V. Panchal, R. Pearce, R. Yakimova, A. Tzalenchuk, and O. Kazakova, Sci. Rep. **3**, 2597 (2013).
5. J. L. Tedesco, B. L. VanMil, R. L. Myers-Ward, J. M. McCrate, S. A. Kitt, P. M. Campbell, G. G. Jernigan, J. C. Culbertson, C. R. Eddy, Jr., and D. K. Gaskill, Appl. Phys. Lett. **95**, 122102 (2009).